Power-Hydraulic Coupling Dynamic Model of the Reciprocating Membrane Pump Used in Fault Diagnosis and the Simulation

Pei-yuan Meng, Kai Liu, and Lin Xu

Abstract Reciprocating membrane pump's fault diagnosis usually needs a dynamic model which can accurately reflect the running state of the system. But the dynamic models of the pump used in the past mostly have a fixed crank angular velocity, and have no consideration of the relations between crank speed, piston pressure, inertia force, etc. In this paper, a new dynamic model of the reciprocating pump include power end and hydraulic ends is founded to solve this problem. The Matlab computed results of the model show that, angular velocity of the crank will keep fluctuating in a limited area after the system become stable, and the fluctuation range with a power fixed input is much smaller then when the input torque is fixed. The results are close to actual experiences and the dynamic model of the reciprocating pump can be used in the further studies of the reciprocating membrane pump's fault diagnosis.

Keywords Coupling • Dynamic • Fault diagnosis • Reciprocating membrane pump • Slider-Crank mechanism

1 Introduction

Reciprocating membrane pump (Fig. 1) is widely used in various industries such as non-ferrous metallurgy, coal, electric power, etc. Ore slurry and hydraulic fluid are separated in the working cavity, so it is especially fit the transportation of substances with high temperature, high concentration or causticity (Ling Xueqin 2006). Reciprocating membrane pump for industrial use is usually working with

P. Meng (✉) • K. Liu • L. Xu
Department of Mechanical and Precision Instrument Engineering, Xi'an University of Technology, Xi'an, China
e-mail: lyg041@163.com

E. Qi et al. (eds.), *Proceedings of 20th International Conference on Industrial Engineering and Engineering Management*, DOI 10.1007/978-3-642-40063-6_21,

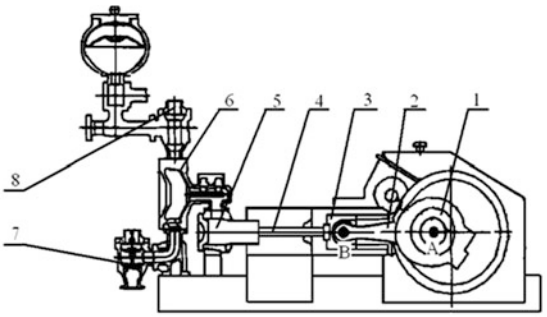

Fig. 1 Constitution of the reciprocating membrane pump. *1* Crankshaft, *2* Linkage, *3* Cross-slider, *4* Piston rod, *5* Piston, *6* Membrane, *7* Feeding valve, *8* Discharge valve

high inertia force and stress, and more importantly, there are coupling relations between the movement factors such as crank speed, piston pressure and so on. Previous studies usually considered the reciprocating membrane pump as a speed fixed system (Qin Wei-xian 2012; Liu Jie et al. 2007; Shi Lichen and Duan Zhishan 2009; Zhang Jinfu et al. 2001; Danielson 2000), and obviously it is not quite suitable for precise dynamic analysis. In this paper, a new dynamic model of the reciprocating pump is put forward to solve the problems.

2 The Model of the Power End

As Fig. 2 shows, the power end of the membrane pump is a kind of Slider-Crank mechanism.

The positive direction of angular rate and angular acceleration is anticlockwise, and the positive direction of linear speed and line acceleration is right. J_0 and J_{S2} are the rotational inertias of the Crank and the Linkage; S_1 and S_2 are the mass center of the Crank and the Linkage.

2.1 Dynamics Equations of the Linkage

Figure 3 shows the force condition of the linkage (Wang Guoqing and Liu Hongzhao 2001). The direction of F_{12}^n is along the crank, the direction of F_{12}^t is perpendicular to the crank. From the Newton second law we can know that:

$$\begin{cases} m_2\ddot{x}_{s2} = -F_{12}^n\cos\theta_1 - F_{12}^t\sin\theta_1 + F_{32}^x & (1) \\ m_2\ddot{y}_{s2} = -F_{12}^n\sin\theta_1 + F_{12}^t\cos\theta_1 + F_{32}^y - m_2 g & (2) \end{cases}$$

Then from the moment equilibrium conditions of the Linkage there is:

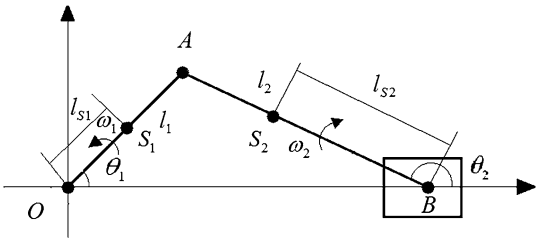

Fig. 2 Power end of the pump

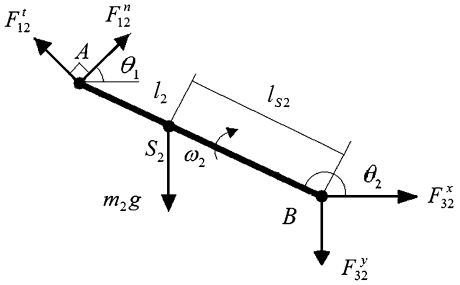

Fig. 3 Force condition of the linkage

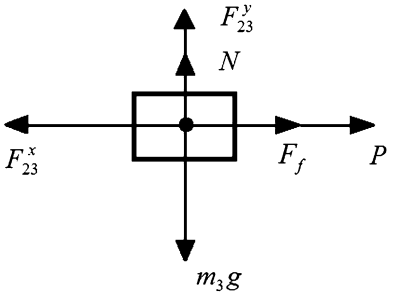

Fig. 4 Force condition of the slider

$$J_{s2}\ddot{\theta}_2 = F_{12}^t (l_2 - l_{s2}) \cos(\theta_2 - \theta_1) + F_{12}^n (l_2 - l_{s2}) \sin(\theta_2 - \theta_1) + F_{32}^x l_{s2} \sin\theta_2 - F_{32}^y l_{s2} \cos\theta_2 \quad (3)$$

Through the kinematic analysis of S_2, we can also know:

$$\begin{cases} \ddot{x}_{s2} = \ddot{x}_3 - \dot{\theta}_2^2 l_{s2} \cos\theta_2 - \ddot{\theta}_2 l_{s2} \sin\theta_2 & (4) \\ \ddot{y}_{s2} = -\dot{\theta}_2^2 l_{s2} \sin\theta_2 + \ddot{\theta}_2 l_{s2} \cos\theta_2 & (5) \end{cases}$$

2.2 Dynamics Equations of the Slider and the Crank Parts

Considered the force condition of the Slider Part (Fig. 4), mark the friction force as F_f and the piston pressure as P. There are relations follows:

$$\begin{cases} N + F_{23}^{y} - m_3 g = 0 & (6) \\ m_3 \ddot{x}_3 = F_{23}^{x} + P + \mu N & (7) \end{cases}$$

From the moment equilibrium conditions of the crank there is:

$$J_0 \ddot{\theta}_1 = T + F_{21}^{t} l_1 - m_1 l_{s1} g \cos\theta_1 \quad (8)$$

In the equation, T is the driving torque of the system.

Because F_{21}^{n} always changes with the motion of the linkage and cannot be confirmed now, so consider it as a intermediate variable.

2.3 Geometric Restraint Equations

Since the Slider-Crank Mechanism will always be a triangle during the motion process, the follow relations must exist (Chen Dewei 2005):

$$\begin{cases} l_1 \cos\theta_1 - l_2 \cos\theta_2 = x & (9) \\ l_1 \sin\theta_1 - l_2 \sin\theta_2 = 0 & (10) \end{cases}$$

Then we can know the relations between the angular velocities and the angular accelerations:

$$\begin{cases} -l_1 \dot{\theta}_1 \sin\theta_1 + l_2 \dot{\theta}_2 \sin\theta_2 = \dot{x}_3 & (11) \\ l_1 \dot{\theta}_1 \cos\theta_1 - l_2 \dot{\theta}_2 \cos\theta_2 = 0 & (12) \end{cases}$$

$$\begin{cases} -l_1 \left(\ddot{\theta}_1 \sin\theta_1 + \dot{\theta}_1^2 \cos\theta_1 \right) + l_2 \left(\ddot{\theta}_2 \sin\theta_2 + \dot{\theta}_2^2 \cos\theta_2 \right) = \ddot{x}_3 & (13) \\ l_1 \left(\ddot{\theta}_1 \cos\theta_1 - \dot{\theta}_1^2 \sin\theta_1 \right) - l_2 \left(\ddot{\theta}_2 \cos\theta_2 - \dot{\theta}_2^2 \sin\theta_2 \right) = 0 & (14) \end{cases}$$

Equations (13) and (14) are usually used to simulate the Slider-Crank Mechanism with fixed rev (Han Zhixin et al. 2006).

2.4 The Dynamical Model of the Power End

Obviously:

$$F_{12}^{n} = -F_{21}^{n} \qquad F_{32}^{x} = -F_{23}^{x}$$
$$F_{12}^{t} = -F_{21}^{t} \qquad F_{32}^{y} = -F_{23}^{y}$$

Through mathematical calculation based on Eqs. (1), (2), (3), (4), (5), (6), (7), (8), (9), (10), (11), (12), (13) and (14), we can finally get the dynamical model of the power end as follow:

$$\begin{cases} A = m_3 l_{s2} \sin\theta_2 (\cos\theta_1 - \mu \sin\theta_1) + (m_2 + m_3)(l_2 - l_{s2}) \sin(\theta_2 - \theta_1) \\ \quad - (m_2 + m_3) l_{s2} \sin\theta_1 (\cos\theta_2 - \mu \sin\theta_2) \\ B = J_{s2} (\cos\theta_1 - \mu \sin\theta_1) - m_2 l_{s2} (l_2 - l_{s2}) \sin(\theta_2 - \theta_1)(\sin\theta_2 + \mu \cos\theta_2) \\ \quad + m_2 l_{s2}^2 \cos(\theta_2 - \theta_1)(\cos\theta_2 - \mu \sin\theta_2) \\ C = (l_2 - l_{s2}) \cos(\theta_2 - \theta_1)(\cos\theta_1 - \mu \sin\theta_1) \\ \quad - (l_2 - l_{s2}) \sin(\theta_2 - \theta_1)(\sin\theta_1 + \mu \cos\theta_1) + l_{s2} (\cos\theta_2 - \mu \sin\theta_2) \\ F = (l_2 - l_{s2}) \sin(\theta_2 - \theta_1)(\sin\theta_2 + \mu \cos\theta_2) \\ \quad - l_{s2} \cos(\theta_2 - \theta_1)(\cos\theta_2 - \mu \sin\theta_2) \\ G = (l_2 - l_{s2}) \sin(\theta_2 - \theta_1) - l_{s2} \sin\theta_1 (\cos\theta_2 - \mu \sin\theta_2) \\ \quad + l_{s2} \sin\theta_2 (\cos\theta_1 - \mu \sin\theta_1) \\ I = (m_2 + m_3)(l_2 - l_{s2}) \mu \sin(\theta_2 - \theta_1) - (m_2 + m_3) l_{s2} \cos\theta_1 (\cos\theta_2 - \mu \sin\theta_2) \\ \quad + m_3 l_{s2} \cos\theta_2 (\cos\theta_1 - \mu \sin\theta_1) \end{cases}$$

$$\begin{cases} \left[-l_1^2 l_2 \sin(\theta_2 - \theta_1) A - l_1^2 B \cos\theta_1 + l_2 J_0 C \cos\theta_2\right] \ddot{\theta}_1 \\ \quad + \left[l_1^2 l_2 A \cos(\theta_2 - \theta_1) + l_1^2 B \sin\theta_1\right] \dot{\theta}_1^2 + \left[- l_1 l_2^2 A \cos 2\theta_2 \right. \\ \quad - l_1 l_2 B \sin\theta_2 + m_2 l_1 l_2^2 l_{s2} \cos\theta_2 \sin(\theta_2 - \theta_1) \left(\cos\theta_2 \right. \\ \quad \left. - \mu \sin\theta_2 \right)] \dot{\theta}_2^2 + l_1 l_2 G P \cos\theta_2 + l_2 C \cos\theta_2 \left(m_1 g \cos\theta_1 \right. \\ \quad \left. - T \right) + l_1 l_2 g I \cos\theta_2 = 0 \\ \left[- l_1^2 l_2 A \sin(\theta_2 - \theta_1) + J_0 l_2 C \cos\theta_2 + m_2 l_1^2 l_{s2} F \cos\theta_1 \right. \\ \quad - J_{s2} l_1^2 \cos\theta_1 (\cos\theta_1 - \mu \sin\theta_1) \left] \ddot{\theta}_2 + \right[- l_1^2 l_2 A \cos(\theta_2 - \theta_1) \\ \quad - J_0 l_2 C \cos\theta_2 + m_2 l_1^2 l_2 l_{s2} \cos\theta_1 \sin(\theta_2 - \theta_1) \left(\cos\theta_2 \right. \\ \quad \left. - \mu \sin\theta_2 \right)] \ddot{\theta}_2^2 + \left(l_1^3 A + J_0 l_1 C \sin\theta_1 \right) \dot{\theta}_1^2 + l_1^2 G P \cos\theta_1 \\ \quad + l_1 \cos\theta_1 (m_1 g \cos\theta_1 - T) H + l_1^2 g I \cos\theta_1 = 0 \end{cases} \tag{15}$$

(16)

3 The Model of the Hydraulic End

From the Bernoulli Equation of the Hydrodynamics, the relations below between Slider-speed and Piston-pressure exist (Zhang Yeying 1999; Zhang Hongjia et al. 2000):

$$\begin{cases} P_1 = \rho g Z_p + P_p + \rho \left[(A_3/A_P)^2 - 1 \right] \dot{x}_3^2/2 & (17) \\ P_2 = \rho g Z_X + P_X + \rho \left[(A_3/A_X)^2 - 1 \right] \dot{x}_3^2/2 & (18) \end{cases}$$

In the equations:

P_1—Piston-pressure when discharging fluid;
P_2—Piston-pressure when imbibing fluid;
P_p—Pressure of the outflow tube;
P_X—Pressure of the inflow tube;
Z_p—Distance between piston and outflow tube;
Z_X—Distance between piston and inflow tube;
A_3—Sectional area of the piston;
A_P—Sectional area of the outflow tube;
A_X—Sectional area of the inflow tube;
ρ—Density of the ore slurry;
$\dot{x}_3$—Speed of the piston;

4 Simulation Analysis of Reciprocating Membrane Pump

Marked Piston-pressure as P, and $\mu > 0$, bring in step functions:

$$\mu\left(\dot{x}_3\right) = \begin{cases} \mu & ; \ \dot{x}_3 < 0 \\ -\mu & ; \ \dot{x}_3 > 0 \end{cases};$$

$$signp_1\left(\dot{x}_3\right) = \begin{cases} 0 & ; \ \dot{x}_3 < 0 \\ -1 & ; \ \dot{x}_3 > 0 \end{cases}; \quad signp_2\left(\dot{x}_3\right) = \begin{cases} 1 & ; \ \dot{x}_3 < 0 \\ 0 & ; \ \dot{x}_3 > 0 \end{cases}$$

Then: $P = signp_1\left(\dot{x}_3\right) \cdot P_1 + signp_2\left(\dot{x}_3\right) \cdot P_2$;

Program the dynamical model of the Reciprocating membrane pump in Matlab and calculate. The basic parameters are:

$m_1 = 5$ kg; $m_2 = 20$ kg; $m_3 = 5$ kg; $l_1 = 0.254$ m; $l_2 = 1.257$ m; $l_{S1} = 0.125$ m; $A_0 = 0.007$ m^2; $A_X = 0.002$ m^2; $A_P = 0.002$ m^2; $Z_X = Z_P = 0.5$ m

4.1 Input Torque Fixed

When input torque is fixed at $30N \cdot M$, the displacements, speeds of the crank and the linkage are shown in Fig. 5.

After the system started, angular velocity of the crank increased, then the system became stable 4 s later. The angular velocity of the crank appeared small scale fluctuant under the influence of the parts' inertia forces and the time varying piston pressure.

When input torque is fixed at $50N \cdot M$, the displacements, speeds of the crank and the linkage are showed in Fig. 6.

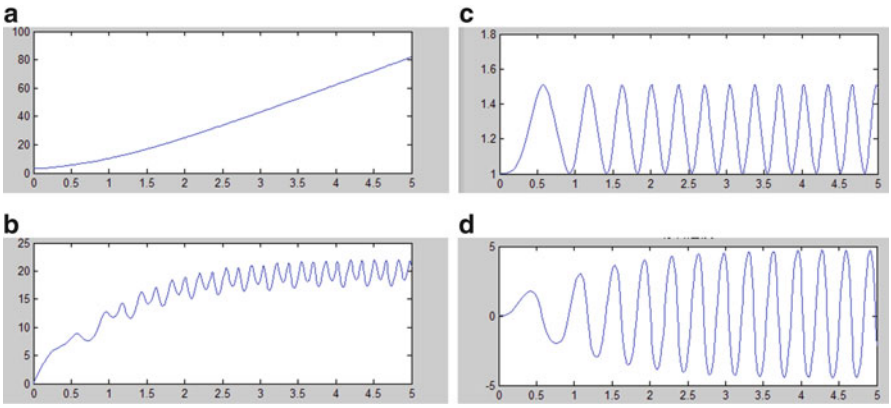

Fig. 5 T = 30 NM (**a**) Crank's rotation (**b**) Crank's angular velocity (**c**) Linkage's displacements (**d**) Linkage's speed

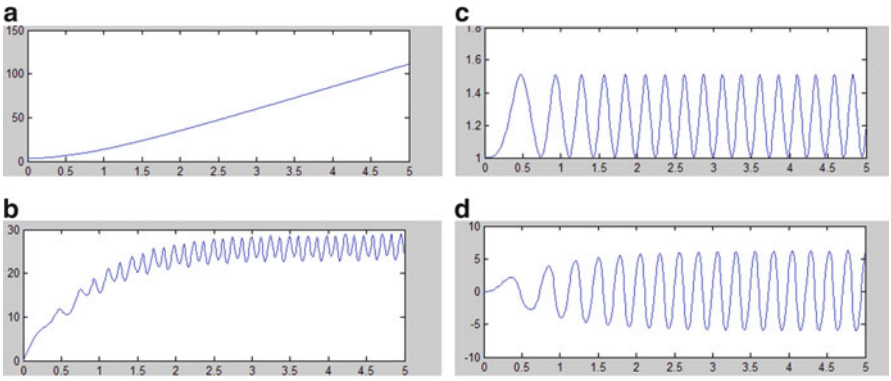

Fig. 6 T = 50 NM (**a**) Crank's rotation (**b**) Crank's angular velocity (**c**) Linkage's displacements (**d**) Linkage's speed

After the system started, angular velocity of the crank increased, then the system became stable 3 s later. Compared with when $T = 30N \cdot M$, the angular velocity fluctuated in a wider area, the vibration frequency was higher, and the vibration circumstance was more severe.

4.2 Input Power Fixed

When input power is fixed at 1.5 KW, the displacements, speeds of the crank and the linkage are showed in Fig. 7.

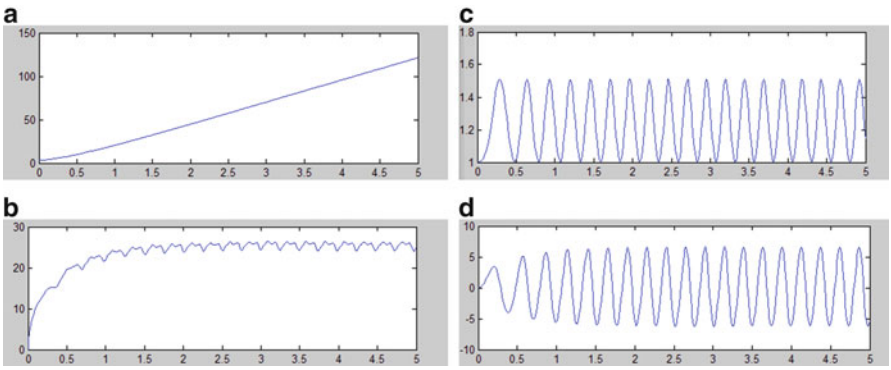

Fig. 7 P = 1.5 kw (**a**) Crank's rotation (**b**) Crank's angular velocity (**c**) Linkage's displacements (**d**) Linkage's speed

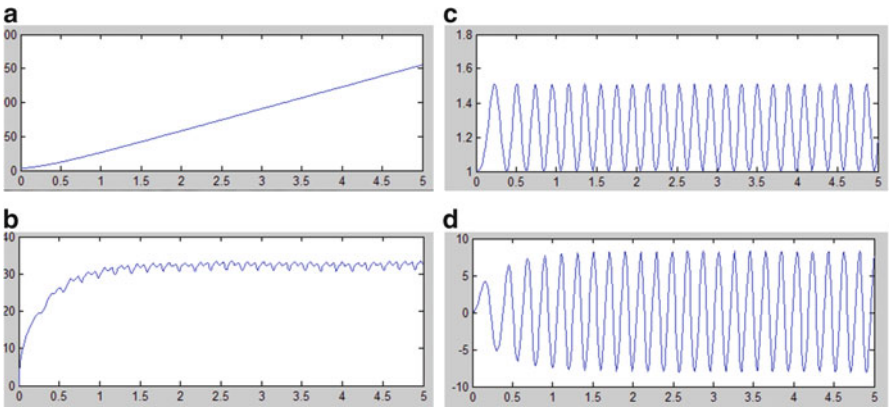

Fig. 8 P = 2.7 kw (**a**) Crank's rotation (**b**) Crank's angular velocity (**c**) Linkage's displacements (**d**) Linkage's speed

After the system started, angular velocity of the crank increased, then the system became stable 2 s later. The angular velocity of the crank also appeared small scale fluctuant under the influence of parts' inertia forces and the time varying piston pressure.

When input power is fixed at 2.7 KW, the displacements, speeds of the crank and the linkage are showed in Fig. 8.

After the system started, angular velocity of the crank increased, then the system became stable 1.5 s later. Compared with when $P = 1.5$ KW, the fluctuation ranges of the angular velocity changed not too much, and the vibration frequency increased as the angular velocity is bigger.

When the pump working in input power fixed condition, the time before the system becomes stable is shorter, the fluctuations of the angular velocity is smaller. The pump can run with smaller vibration and stable.

5 Conclusion

1. This article put forward a new dynamic model of the reciprocating pump considering coupling relations between the movement factors, such as crank speed, piston pressure and so on, then calculated the model with fixed power input and fixed torque input.
2. Before the pump become stable operation there is a certain amount of time. When the system became stable, the angular velocity and acceleration will fluctuate in a area.
3. Compared with the torque fixed input, the fluctuations range of the angular velocity and acceleration are much smaller when the input power is fixed. Also, the time before stabilization is shorter, the pump will run with a smaller vibration.
4. The results are close to actual experiences and the dynamic model of the reciprocating pump can be used in the further studies of the reciprocating membrane pump's fault diagnosis.

References

Chen Dewei (2005) Simulation of slider-crank mechanism based on Matlab (in Chinese). J Taiyuan Univ Sci Technol 26(3):172–175

Danielson P (2000) Diaphragm pump designs determine results. R&D Mag 42(11):59–61

Han Zhixin, Shi Wenrui, Lu Xuehong (2006) Effect on dynamic character of internal combustion engine by different length parameters of crank slide mechanism (in Chinese). Coal Mine Mach 27(3):435–437

Ling Xueqin (2006) Core technologies and technical references of the reciprocating membrane pump (in Chinese). Dev Innov Mach Electr Prod 19(5):45–48

Liu Jie, Li Chaofeng, Wen Bangchun (2007) Dynamic properties analysis of the diaphragm pump based on virtual prototype (in Chinese). J Mech Transm 31(2):1–4

Qin Wei-xian (2012) Dynamic model of the reciprocating pump's crank-link mechanism and analysis (in Chinese). J Mech Transm 36(3):70–73

Shi Lichen, Duan Zhishan (2009) Dynamic modelling and analysis on loose joint of crank slider mechanism of membrane pump (in Chinese). J Mach Des Tianjin 26:40–43

Wang Guoqing, Liu Hongzhao (2001) Dynamic response of slider-crank mechanism with clearance (in Chinese). Trans Chin Soc Agric Mach 32(6):5–7

Zhang Hongjia, Huang Yi, Wang Jiwei (2000) Hydraulic and pneumatic drive. China Machine Press, Beijing

Zhang Jinfu, Xu Qingyu, Zhang Ling (2001) Dynamic modeling and calculation of slider-crank mechanism with flexible connecting rod and viscous friction (in Chinese). Acta Aeronautica et Astronautica Sinica 22(3):274–276

Zhang Yeying (1999) Hydromechanics. Higher Education Press, Beijing, pp 143–163